Journal of Experimental Botany, Vol. 61, No. 13, pp. 3647–3662, 2010
doi:10.1093/jxb/erq178 Advance Access publication 30 June, 2010
This paper is available online free of all access charges (see http://jxb.oxfordjournals.org/open_access.html for further details)

Journal of Experimental Botany
www.jxb.oxfordjournals.org

RESEARCH PAPER

Revealing diversity in structural and biochemical forms of C_4 photosynthesis and a C_3–C_4 intermediate in genus *Portulaca* L. (Portulacaceae)

Elena V. Voznesenskaya[1], Nuria K. Koteyeva[1], Gerald E. Edwards[2,*] and Gilberto Ocampo[3,†]

[1] Laboratory of Anatomy and Morphology, V.L. Komarov Botanical Institute of the Russian Academy of Sciences, Prof. Popov Street 2, 197376, St. Petersburg, Russia
[2] School of Biological Sciences, Washington State University, Pullman, WA 99164-4236, USA
[3] Rancho Santa Ana Botanic Garden, 1500 North College Avenue, Claremont, CA 91711, USA

[†] Present address: California Academy of Sciences, 55 Music Concourse Drive, Golden Gate Park, San Francisco, CA 94118, USA
* To whom correspondence should be addressed: E-mail: edwardsg@wsu.edu

Received 12 February 2010; Revised 24 May 2010; Accepted 28 May 2010

Abstract

Portulacaceae is one of 19 families of terrestrial plants in which species having C_4 photosynthesis have been found. Representative species from major clades of the genus *Portulaca* were studied to characterize the forms of photosynthesis structurally and biochemically. The species *P. amilis*, *P. grandiflora*, *P. molokiniensis*, *P. oleracea*, *P. pilosa*, and *P. umbraticola* belong to the subgenus *Portulaca* and are C_4 plants based on leaf carbon isotope values, Kranz anatomy, and expression of key C_4 enzymes. *Portulaca umbraticola*, clade Umbraticola, is NADP-malic enzyme (NADP-ME)-type C_4 species, while *P. oleracea* and *P. molokiniensis* in clade Oleracea are NAD-ME-type C_4 species, all having different forms of Atriplicoid-type leaf anatomy. In clade Pilosa, *P. amilis*, *P. grandiflora*, and *P. pilosa* are NADP-ME-type C_4 species. They have Pilosoid-type anatomy in which Kranz tissues enclose peripheral vascular bundles with water storage in the centre of the leaf. *Portulaca* cf. *bicolor*, which belongs to subgenus *Portulacella*, is an NADP-ME C_4 species with Portulacelloid-type anatomy; it has well-developed Kranz chlorenchyma surrounding lateral veins distributed in one plane under the adaxial epidermis with water storage cells underneath. *Portulaca cryptopetala* (clade Oleracea), an endemic species from central South America, was identified as a C_3–C_4 based on its intermediate CO_2 compensation point and selective localization of glycine decarboxylase of the photorespiratory pathway in mitochondria of bundle sheath cells. The C_4 *Portulaca* species which were examined also have cotyledons with Kranz-type anatomy, while the stems of all species have C_3-type photosynthetic cells. The results indicate that multiple structural and biochemical forms of C_4 photosynthesis evolved in genus *Portulaca*.

Key words: C_3 plants, C_3–C_4 intermediate, C_4 plants, chloroplast ultrastructure, immunolocalization, NAD-ME-type, NADP-ME-type, photosynthetic enzymes, *Portulaca*, Portulacaceae.

Introduction

Most terrestrial plants have C_3-type photosynthesis, in which there is direct fixation of atmospheric CO_2 via ribulose bisphosphate carboxylase oxygenase (Rubisco) in all chloroplast-containing leaf mesophyll (M) tissues. Only ~3% of terrestrial species are C_4 plants in which atmospheric CO_2 is fixed initially in the C_4 cycle by

Abbreviations: BS, bundle sheath; $\delta^{13}C$ value, a measure of the carbon isotope composition; CAM, Crassulacean acid metabolism; Γ, CO_2 compensation point; Γ^*, CO_2 compensation point based on Rubisco carboxylase/oxygenase activity; GDC, glycine decarboxylase; M, mesophyll; NAD-ME, NAD-malic enzyme; NADP-ME, NADP-malic enzyme; PEPC, phosphoenolpyruvate carboxylase; PEP-CK, phosphoenolpyruvate carboxykinase; PPDK, pyruvate, Pi dikinase; PPFD, photosynthetic photon flux density; Rubisco, ribulose bisphosphate carboxylase oxygenase; VB, vascular bundle.

phosphoenolpyruvate carboxylase (PEPC) located in M cells. This leads to the formation of C_4 acids which act as donors of CO_2 to Rubisco in bundle sheath (BS) cells. Through this CO_2-concentrating mechanism which represses photorespiration, C_4 plants are recognized as having an increased capacity for carbon assimilation and higher efficiency in nitrogen and water use in warm climates. For this reason, there is interest in genetically modifying major C_3 crops with C_4 traits to reduce photorespiration, and in developing the use of C_4 species for production of biofuels (Brown, 1999; Samson *et al.*, 2005; Sheehy *et al.*, 2007). The main structural difference associated with this pathway in most C_4 species is the specialized leaf anatomy (called Kranz type) with close coordination of function between two types of cells surrounding vascular bundles (VBs), the enlarged chlorenchymatous BS cells and the radially arranged M cells (Edwards and Walker, 1983; Hatch, 1987; Kanai and Edwards, 1999; Edwards and Voznesenskaya, 2010). C_4 photosynthesis has been found in 19 families of angiosperm plants, 16 of which correspond to dicot lineages (Sage, 2004).

In the order Caryophyllales there are 23 families (Thorne and Reveal, 2007); eight of them have species with C_4 photosynthesis: Aizoaceae, Amaranthaceae, Caryophyllaceae, Gisekiaceae, Molluginaceae, Nyctaginaceae, Polygonaceae, and the non-monophyletic Portulacaceae (Sage, 2004). In Portulacaceae, which has 29 genera as traditionally circumscribed (Eggli, 2002; but see Nyffeler and Eggli, 2010 for an alternative circumscription), only *Portulaca* is known to have C_4 species. Previous suggestions that some species of *Anacampseros* and *Grahamia* may be C_4 are not supported by a recent study (Guralnick *et al.*, 2008), which indicates the occurrence of Crassulacean acid metabolism (CAM) rather than C_4 photosynthesis in these genera.

For many years *Portulaca oleracea* L. has been recognized as an example of a dicot having C_4 photosynthesis with an NAD-malic enzyme (NAD-ME)-type C_4 cycle and Kranz anatomy with well-developed grana in BS cell chloroplasts (Laetsch, 1971; Gutierrez *et al.*, 1974; Laetsch, 1974; Carolin *et al.*, 1978; Sprey and Laetsch, 1978). In contrast, *P. grandiflora* Hook. is known to be an NADP-malic enzyme (NADP-ME)-type C_4 species with agranal BS chloroplasts (Gutierrez *et al.*, 1974; Carolin *et al.*, 1978). This raises the question of how much diversity in forms of photosynthetic types exists within the genus. The number of species in the genus is uncertain, but some authors estimate there are >100 (Poellnitz, 1934; Legrand, 1958) which are distributed in the tropics and subtropics, with centres of diversity in South America and Africa. The most widely accepted classification of *Portulaca* was proposed by Geesink (1969), who recognized two subgenera, *Portulaca* and *Portulacella*, although DNA sequence data analysis shows that both subgenera warrant recircumscription in order to keep them monophyletic (G Ocampo and JT Columbus, unpublished). The goal of this work was to identify and characterize different anatomical and biochemical forms of photosynthesis in *Portulaca*. Evidence was obtained for a C_3–C_4 intermediate species having reduced photorespiration and lacking Kranz anatomy, and occurrence of three major forms of Kranz anatomy and two C_4 biochemical subtypes.

Materials and methods

Plant material

Seeds of *P. oleracea* L. were collected in Pullman, WA. Seeds of other species of the genus *Portulaca* were obtained from the following sources: *P. amilis* Speg. (Kew Royal Botanic Gardens, #6541, misnamed as *P. pilosa* L.), *P. cryptopetala* Speg. (Kew Royal Botanic Gardens, #8350), *P. grandiflora* Hook. (Lilly Miller, The Chas. H. Lilly Co., Portland), *P. pilosa* L. (greenhouse plant collection, Komarov Botanical Institute, St. Petersburg), and *P. umbraticola* Kunth. cv. 'wildfire mixed' (Philippines, plant market). Seeds of *P. molokiniensis* were kindly provided by F. Okamoto, Pearl City, Hawaii. Small cuttings of *P.* cf. *bicolor* F. Muell. (Ocampo *et al.* 1726, BRI, RSA) were taken from individuals (~1.5 years old) maintained in cultivation at Rancho Santa Ana Botanic Garden, Claremont, CA, USA.

All seeds were stored at 3–5 °C prior to use and were germinated on the surface of potting soil (Sunshine LC-1 from SUNGRO Horticulture, Bellevue, WA, USA) at 25 °C and a photosynthetic photon flux density (PPFD) of 100 µmol quanta m^{-2} s^{-1}. The seedlings were then transplanted to soil in 10 cm diameter pots (one seedling per pot). After ~1 week, established plants were transferred to a growth chamber (model GC-16; Enconair Ecological Chambers Inc., Winnipeg, Canada) and grown under a PPFD of ~400 µmol quanta m^{-2} s^{-1} with a 16/8 h light/dark photoperiod and 25/18 °C day/night temperature regime. Plants were fertilized once per week with Peter's Professional (20:20:20; Scotts Miracle-Gro). For microscopy and biochemical analyses, samples of mature leaves and stem segments were taken from ~2.5- to 3-month-old plants. Cotyledons were fixed ~2 weeks after germination when the first leaves were already established. *Sesuvium portulacastrum* (L.) L. (Aizoaceae) was collected in Honolulu (Hawaii) and grown from cuttings in the same growth chamber; it was used as a representative C_3 species having flattened succulent leaves. *Spartina anglica* C. E. Hubb. (Poaceae) was collected in Livingston Bay, Washington, USA, and maintained under greenhouse conditions with a maximum PPFD of ~1200 µmol quanta m^{-2} s^{-1} and temperature near 33/21 °C day/night. This species was used as a representative phosphoenolpyruvate carboxykinase (PEP-CK)-type for western blot analysis.

Voucher specimens are available at the Marion Ownbey Herbarium, Washington State University: *P. amilis* (WS377960), *P. cryptopetala* (WS377956), *P. grandiflora* (WS377953), *P. oleracea* (WS377954), *P. pilosa* (WS377958), *P. umbraticola* (WS377957), *P.* cf. *bicolor* (WS377959), and *S. portulacastrum* (WS377955).

Light and electron microscopy

Hand cross-sections of fresh leaves and stems were placed in water and studied under a stereo light microscope (Wild Heerbrugg, Switzerland) equipped with the LM Digital Camera & Software (Jenoptik ProgRes Camera, C12plus, Jena, Germany) or under UV light [with a 4',6-diamidino-2-phenylindole (DAPI) filter] on a Leica Fluorescence Microscope Leica DMFSA (Leica Microsystems Wetzlar GmbH, Germany).

For structural studies, 2–3 samples were taken from 2–3 plants for each species from cotyledons, the middle part of the leaf, and young stems 1–4 cm from the tip of the shoot. They were fixed at 4 °C in 2% (v/v) paraformaldehyde and 2% (v/v) glutaraldehyde in 0.1 M phosphate buffer (pH 7.2), post-fixed in 2% (w/v) OsO_4, and then, after a standard acetone dehydration procedure, embedded

in Spurr's epoxy resin. Cross-sections were made on a Reichert Ultracut R ultramicrotome (Reichert-Jung GmbH, Heidelberg, Germany). For light microscopy, semi-thin sections were stained with 1% (w/v) toluidine blue O in 1% (w/v) $Na_2B_4O_7$, and studied under the Olympus BH-2 (Olympus Optical Co., Ltd) light microscope equipped with the LM Digital Camera & Software (Jenoptik ProgRes Camera, C12plus, Jena, Germany). Ultra-thin sections were stained for transmission electron microscopy with 4% (w/v) uranyl acetate followed by 2% (w/v) lead citrate. Hitachi H-600 and JEOL JEM-1200 EX transmission electron microscopes were used for observation and photography.

In situ *immunolocalization*

Leaf samples were fixed at 4 °C in 2% (v/v) paraformaldehyde and 1.25% (v/v) glutaraldehyde in 0.05 M PIPES buffer, pH 7.2. The samples were dehydrated with a graded ethanol series and embedded in London Resin White (LR White, Electron Microscopy Sciences, Fort Washington, PA, USA) acrylic resin. The antibody used (raised in rabbit) was anti-*Pisum sativum* glycine decarboxylase (GDC) IgG which was prepared against the P-protein subunit (courtesy of Dr. David Oliver). Pre-immune serum was used as a control.

For transmission electron microscopy immunolabelling, thin sections (~70–90 nm) on Formvar-coated nickel grids were incubated for 1 h in TBST+BSA (TRIS-buffered saline–Tween+bovine serum albumin) to block non-specific protein binding on the sections. They were then incubated for 3 h with either the pre-immune serum diluted in TBST+BSA or anti-GDC (1:10) antibodies. After washing with TBST+BSA, the sections were incubated for 1 h with protein A–gold (15 nm) diluted 1:100 with TBST+BSA. The sections were washed sequentially with TBST+BSA, TBST, and distilled water, and then post-stained with a 1:3 dilution of 0.5% (w/v) potassium permanganate and 2% (w/v) uranyl acetate. Images were collected using a Jeol JEM 1200 EX transmission electron microscope with a MegaView III Camera and Soft Imaging System (Lakewood, CO, USA). The density of labelling was determined by counting the gold particles on electron micrographs and calculating the number per mitochondria (GDC) or per the rest of the cell (background) unit area (1 μm^2). For each cell type, replicate measurements were made on parts of cell sections (n=10–60).

Western blot analysis

Total soluble proteins were extracted from leaves by homogenizing 0.2 g of tissue in 0.5 ml of extraction buffer [100 mM TRIS-HCl, pH 7.5, 10 mM (w/v) $MgCl_2$, 1 mM (w/v) EDTA, 15 mM (v/v) β-mercaptoethanol, 20% (v/v) glycerol, and 1 mM phenylmethylsulphonyl fluoride]. After centrifugation at 10 000 *g* for 10 min in a microcentrifuge, the supernatant was collected and the protein concentration was determined with Bradford protein assay (Bio-Rad) using BSA as a standard. The supernatant fraction was diluted 1:1 in 60 mM TRIS-HCl, pH 7.5, 4% (w/v) SDS, 20% (v/v) glycerol, 0.5% (v/v) β-mercaptoethanol, and 0.1% (w/v) bromophenol blue, and boiled for 5 min for SDS–PAGE. Protein samples (20 μg) were separated by 10% SDS–PAGE, blotted onto nitrocellulose, and probed with anti-*Amaranthus hypochondriacus* NAD-ME IgG which was prepared against the 65 kDa α subunit, courtesy of J Berry (Long and Berry 1996) (1:2000), anti-*Zea mays* 62 kDa NADP-ME IgG, courtesy of C Andreo (Maurino *et al.*, 1996) (1:2500), commercially available anti-*Zea mays* PEPC IgG (1:100 000)(Chemicon, Temecula, CA, USA), anti-*Z. mays* pyruvate,Pi dikinase (PPDK) IgG, courtesy of T Sugiyama (1:50 000), anti-*Nicotiana tabacum* Rubisco large subunit IgG, courtesy of R Chollet (1:10 000), or anti-*Urochloa maxima* PEP-CK, courtesy of R Walker (1:5000) overnight at 4 °C. Goat anti-rabbit IgG–alkaline phosphatase conjugate antibody (Bio-Rad) was used at a dilution of 1:20 000 for detection. Bound antibodies were localized by developing the blots with 20 mM nitroblue tetrazolium and 75 mM 5-bromo-4-chloro-3-indolyl phosphate in detection buffer (100 mM TRIS-HCl, pH 9.5, 100 mM NaCl, 5 mM $MgCl_2$). As control for PEP-CK biochemical type, protein extracts from leaves of *S. anglica* C.E. Hubb. were used.

Measurements of rates of photosynthesis

For measurement of the response of photosynthesis to varying CO_2, and for determining the CO_2 compensation point (Γ), and (Γ*) based on Rubisco carboxylase/oxygenase activity, gas exchange was measured with the FastEst gas system (Laisk and Edwards, 1997; Sun *et al.*, 1999). A leaf was enclosed in a small leaf chamber (3 cm×3 cm×0.5 cm) with an open gas flow rate of 0.5 mmol s^{-1}. The chamber temperature was maintained at 25 °C, with the water jacket of the chamber connected to a thermostated water bath. The upper side of the leaf was illuminated with a PPFD of 900 μmol quanta m^{-2} s^{-1} at the glass window by fibre optics with a Schott KL1500 source (H. Walz, Effeltrich, Germany). PPFD was measured with a Li-Cor-185 quantum sensor. The relative humidity in the leaf chamber was controlled by diverting part of the air flow stream through air that was equilibrated with water at 50 °C. CO_2 and O_2 partial pressures were obtained by mixing pure CO_2, O_2, N_2, and CO_2-free air with the help of capillaries. The pressure difference in the capillaries was stabilized by manostats (tubes with open ends submerged in water to adjustable heights). The water vapour pressure was measured with a psychrometer. CO_2 exchange was measured with an MK3-225 IR gas analyser (ADC, Hoddesdon, Hertfordshire, UK). Data were recorded by computer using an A/D board ME-30 and a RECO program, and analysed by computer programs ANAL and SYNTE. The programs RECO and ANAL were written by V Ova (University Tartu, Estonia) in Turbo-Pascal. The intercellular CO_2 concentration in the leaf was calculated with inputs for the rate of photosynthesis, the CO_2 concentration in the air, and the diffusive resistance of CO_2 from the atmosphere to the intercellular space. The latter is calculated by determining the diffusive resistance to water by measuring transpiration, and the water vapour concentration difference from the leaf to air; for a description see Ku *et al.* (1977) and von Caemmerer and Farquhar (1981).

Two methods were used to measure the CO_2 compensation point. In the conventional method, Γ was determined at a PPFD of 900 μmol quanta m^{-2} s^{-1} and 25 °C by extrapolation of the initial slope of rates of CO_2 fixation (A) versus the intercellular CO_2 concentration in the leaf (C_i) through the x-axis where the net rate of CO_2 assimilation equals zero. In the other method, Γ* was measured as described by Brooks and Farquhar (1985) by taking the co-ordinates of the intersection of CO_2 response curves measured at different light levels. This is considered to correct for any CO_2 evolution from respiratory processes not associated with Rubisco. It provides a more direct measure of the CO_2 compensation point based on Rubisco function with respect to carboxylase versus oxygenase activity.

The area of leaf exposed to incident light was calculated by taking a digital image of the part of the leaf that was enclosed in the chamber, and then determining the exposed leaf area using an Image Analysis program (UTHSCSA, Image Tool for Windows, version 3.00, University of Texas Health Science Center, San Antonio, TX, USA).

Chlorophyll assay

Chlorophyll was extracted in 100% ethanol, and analysed as described in Porra *et al.* (1989). Absorbance was measured at 649 nm and 665 nm on a Graphicord UV-240 Shimadzu spectrophotometer with 4–6 replicates per species. Chlorophyll per unit area was determined by taking the area of the organ (leaf or stem)

exposed to incident light, which was calculated as described above using an Image Analysis program.

Scanning electron microscopy

Observations and capturing images of the epidermal surfaces of live leaves and stems were made using the low vacuum mode on FEI SEM Quanta 200F (FEI Company, Field Emission Instruments, Hillsboro, OR, USA).

$\delta^{13}C$ values

$\delta^{13}C$ values, a measure of the carbon isotope composition, were determined at Washington State University on leaf samples taken from plants using a standard procedure relative to PDB (Pee Dee Belemnite) limestone as the carbon isotope standard (Bender *et al.*, 1973). Plant samples were dried at 80 °C for 24 h, milled to a fine powder, and then 1–2 mg were placed into a tin capsule and combusted in a Eurovector elemental analyser. The resulting N_2 and CO_2 gases were separated by gas chromatography and admitted into the inlet of a Micromass Isoprime isotope ratio mass spectrometer (IRMS) for determination of $^{13}C/^{12}C$ ratios. $\delta^{13}C$ values were calculated where $\delta^{13}C=1000\times(R_{sample}/R_{standard})-1$, where $R=^{13}C/^{12}C$.

Statistical analysis

Where indicated, standard errors were determined, and analysis of variance (ANOVA) was performed with Statistica 7.0 software (StatSoft, Inc.). Tukey's HSD (honest significant difference) tests were used to analyse differences between leaf parameters and species. All analyses were performed at $P<0.05$.

Results

General view of plants and leaf structure

Five of the species studied, *P. umbraticola* (Fig. 1A), *P. oleracea* (Fig. 1D), *P. amilis* (Fig. 1J), *P. cryptopetala* (Fig. 1P), and *P. molokiniensis* (not shown), have flattened obovate leaves; *P.* cf. *bicolor* (Fig. 1M) has flattened, widely ovate to orbicular leaves; *P. grandiflora* (Fig. 1G) and *P. pilosa* (not shown) have lanceolate semi-terete to cylindrical leaves. On handmade cross-sections the distribution of VBs in leaves with different anatomical types is clearly observed. Thus, in flattened leaves of *P. umbraticola* (Fig. 1B) all VBs are surrounded by two layers of chlorenchyma, characteristic of C_4 plants, with specialized chlorenchymatous BS cells and radially arranged palisade M cells, which are distributed in a horizontal lateral plane, with hypodermal layers under the adaxial and abaxial epidermis. The distribution of chlorenchyma can be observed clearly under UV fluorescence, which shows a low level of chlorophyll in hypodermal cells compared with the Kranz chlorenchyma (Fig. 1C).

The features of leaves of *P. oleracea* (Fig. 1E) and *P. molokiniensis* (not shown) are similar to those of *P. umbraticola* including laterally arranged VBs surrounded by two layers of chlorenchyma with layers of hypodermal cells under both epidermal layers. However, in *P. oleracea* and *P. molokiniensis* the small VBs are not distributed in a linear plane; rather, they are in a zig-zag pattern accompanied by unequal development of the hypodermal cells. Further study showed that veins having a different order have a different position; the higher order veins are located closer to adaxial epidermis. Figure 1F shows the distribution of chlorenchyma in a leaf of *P. oleracea*, with most chlorophyllous cells around VBs and with the hypoderm having very few chloroplasts.

Portulaca grandiflora (Fig. 1G, H) and *P. pilosa* (not shown) have very similar semi-terete leaves with a peripheral distribution of individual VBs, surrounded by specialized chlorenchyma layers. The main vein, which is located more or less in the centre of the leaf, is surrounded by water storage tissue. Water storage tissue is also located between the peripheral VBs. In this leaf structure, chlorenchymatous tissues are confined to cell layers surrounding VBs (Fig. 1I), with a higher development of palisade M cells, and sometimes closer positioning of VBs, on the adaxial side of the leaf (not shown). *Portulaca amilis* has a similar distribution of VBs around the leaf periphery, but in the flattened leaf of this species there are 2–3 layers of water storage cells in the middle of the leaf blade between the adaxial and abaxial VBs (Fig. 1K, L). In *P. grandiflora*, there is a hypodermal layer of cells which is often more pronounced on the abaxial side of the leaf, whereas neither *P. pilosa* nor *P. amilis* has a hypodermal layer.

Portulaca cf. *bicolor* (Fig. 1M) has very small flattened leaves, with all VBs (including the main vein) having Kranz chlorenchyma cells distributed just under the adaxial epidermis. There are 5–6 layers of water storage cells on the abaxial side of the leaf, with a slight decrease in layers towards the lateral sides, and no hypodermal layer (Fig. 1N, O).

A totally different type of anatomy was found in flattened leaves of *P. cryptopetala* (Fig. 1P) which clearly have the C_3-like dorsoventral type of anatomy with chlorenchyma distributed evenly throughout the leaf blade, with two layers of palisade-like cells on the adaxial side of the leaf and generally three layers of spongy parenchyma on the abaxial side (Fig. 1Q, R).

Light and electron microscopy

Study by light microscopy further shows differences in the distribution of minor VBs in leaves of the studied species and reveals additional features. In three of the species having flattened leaves, *P. umbraticola*, *P. oleracea* (Fig. 2A, E), and *P. molokiniensis* (not shown), the VBs are situated in the central part of the leaf, and delineated by one layer of hypoderm on the adaxial side and 1–2 layers of hypodermal cells on the abaxial side of the leaf. All lateral VBs are completely surrounded by specialized chlorenchyma layers, BS and M cells (Fig. 2A, E), while two chlorenchyma layers are present only on the adaxial side of the main veins (not shown). In these species, chloroplasts are located in a centripetal position in BS cells, and organelles have a similar concentration in all cells around the VBs (Fig. 2B, F). In *P. umbraticola*, BS chloroplasts are nearly agranal with only a few small grana (Fig. 2C), while M chloroplasts have well-developed grana (Fig. 2D). In contrast, BS cells in

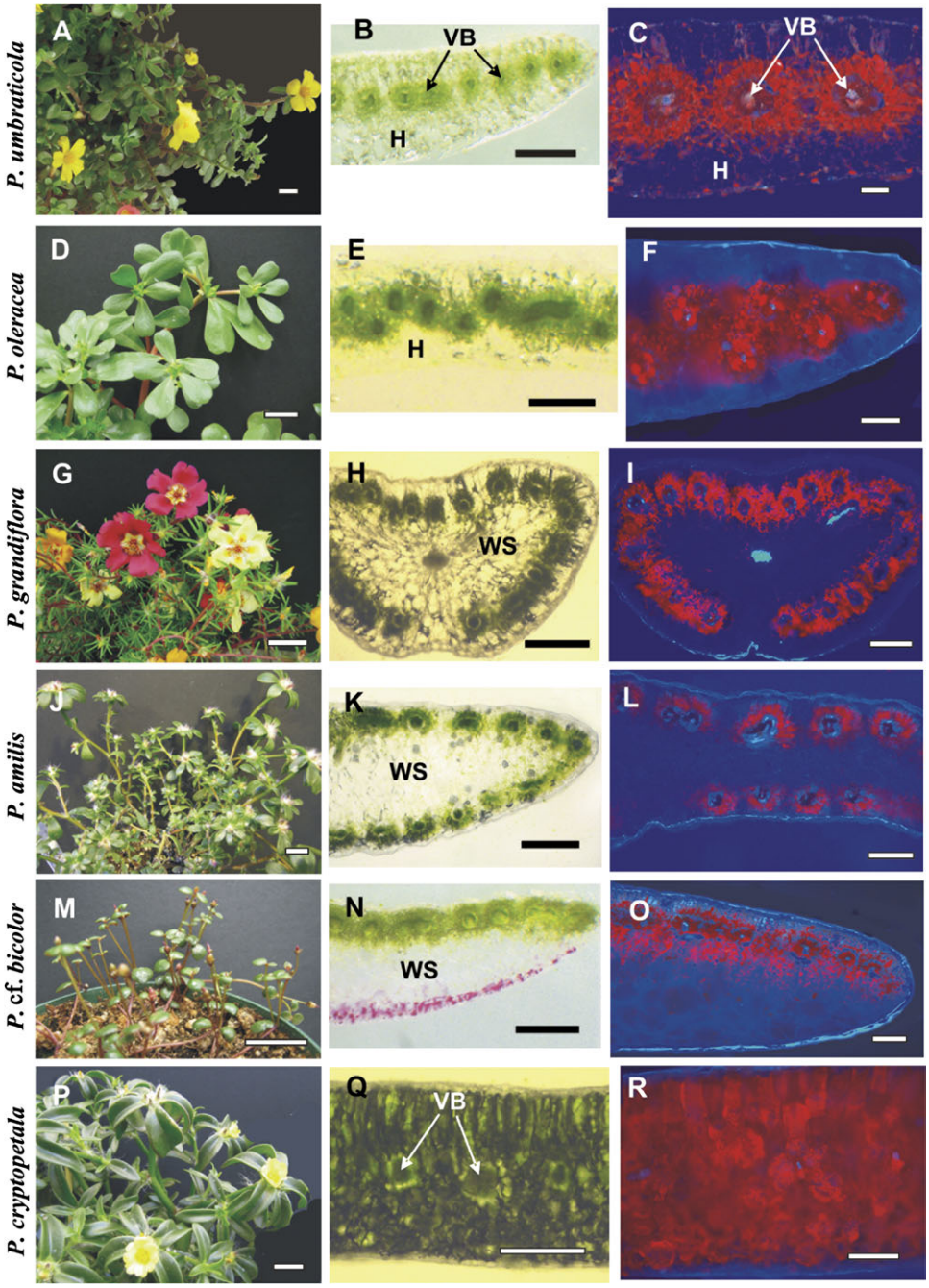

Fig. 1. General view of *Portulaca* species (left panels), hand-made leaf cross-sections (middle panels), and distribution of chlorenchyma under the fluorescent microscope (right panels). (A–C) *Portulaca umbraticola*; (B) distribution of vascular bundles (VBs) in the median paradermal plane; (C) red fluorescence from chlorenchyma is distributed around each VB. (D–F) *Portulaca oleracea*; (E) zig-zag pattern in the distribution of VBs with their positioning in two paradermal levels, (F) fluorescent chlorenchyma surrounds the VBs. (G–I) *Portulaca grandiflora* and (J–L) *P. amilis*; (H, K) VBs are distributed around the leaf periphery, (I, L) chlorenchymatous cells are mostly on the outer side of the VBs. (M–O) *Portulaca* cf. *bicolor*; (N) VBs are only on the adaxial side, (O) chlorophyll fluorescence occurs on the adaxial and abaxial sides of VBs. (P–R) *Portulaca cryptopetala*; (Q) C_3-like dorsoventral type of anatomy, (R) chlorenchyma is distributed evenly in leaf section. H, hypoderm; VB, vascular bundles; WS, water storage tissue. Scale bars: 2 cm for A, D, G, J, M, P; 500 μm for B, E, H, K, N, Q; 250 μm for C, F, I, L, O, R.

P. oleracea contain chloroplasts with well-developed grana and numerous large mitochondria (Fig. 2G), while M chloroplasts are grana deficient (Fig. 2H).

In three species with C_4 anatomy that have VBs distributed around the periphery of the leaf, *P. grandiflora* (Fig. 2I), *P. pilosa* (not shown), and *P. amilis* (Fig. 2M), BS cells surround the minor veins. However, on the interior side of the VBs, where BS cells are adjacent to the phloem part of the bundle on one side and water storage cells on the other side, the BS cells tend to have fewer chloroplasts

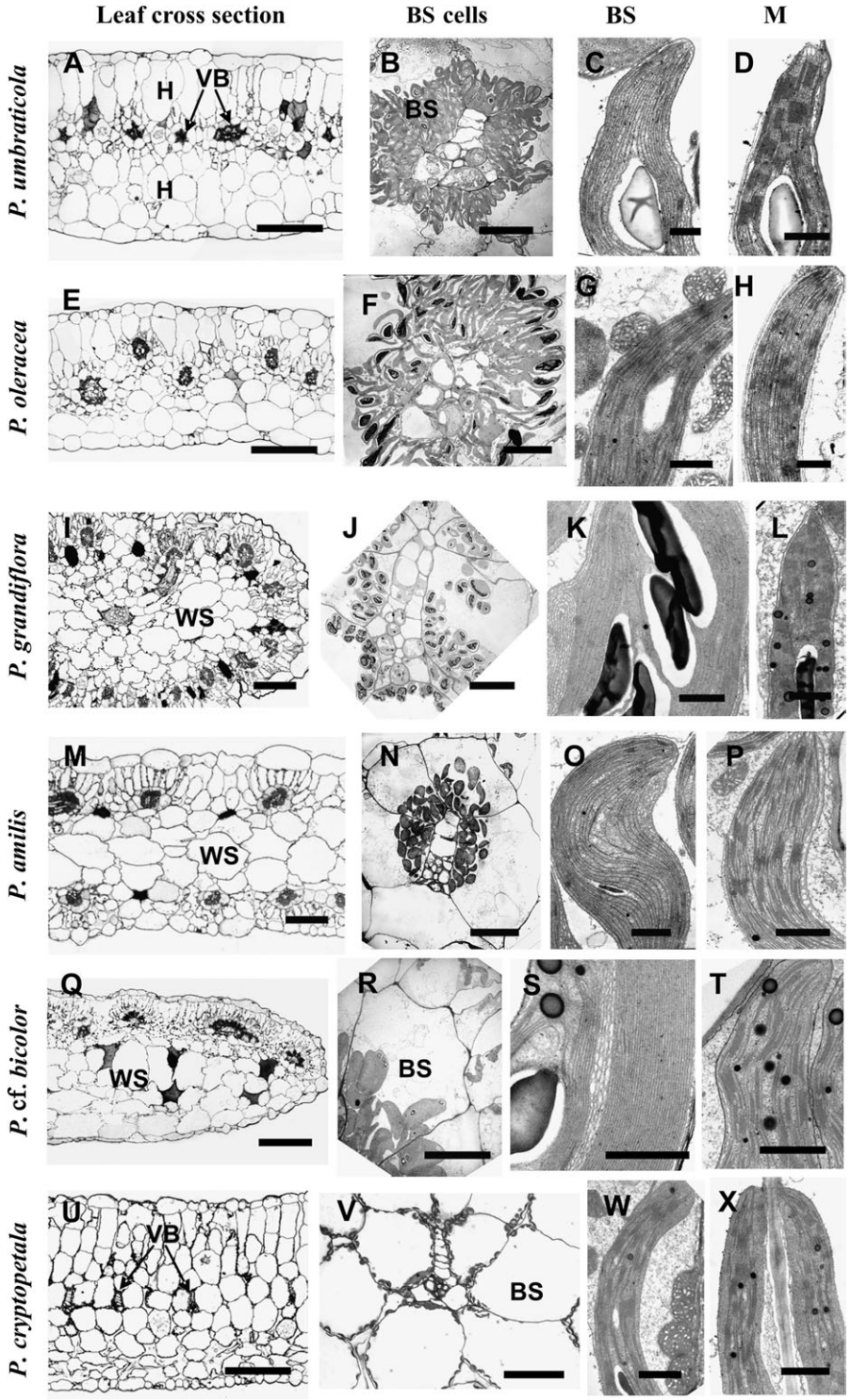

Fig. 2. Light microscopy of leaf cross-sections, electron microscopy of bundle sheath (BS) cells and of chloroplasts and mitochondria in chlorenchyma cells in *Portulaca* species. (A–D) *Portulaca umbraticola*. (E–H) *Portulaca oleracea.* (I–L) *Portulaca grandiflora*. (M–P) *Portulaca amilis*. (Q–T) *Portulaca* cf. *bicolor.* (U–X) *Portulaca cryptopetala*. A, E, I, M, Q, U left panels: light microscopy. B, F, J, N, R, V: BS cells with centripetal positioning of organelles surrounding VBs. BS chloroplasts: (C, K, O, S) grana-deficient (G, W) with well-developed grana and numerous mitochondria. M chloroplasts: (D, L, P, T, X) with well-developed grana and (H) deficient in grana. BS, bundle sheath; H, hypoderm; M, mesophyll; VB, vascular bundle; WS, water storage tissue. Scale bars: 250 μm for A, E, I, M, Q, U; 20 μm for B, F, J, N, R; 100 μm for V; 1 μm for C, D, G, H, K, L, O, P, S, T, W, X.

(Fig. 2N). Palisade M cells are only in contact with BS cells on the external and lateral sides of the VBs, while the internally located BS cells do not have contact with M cells. In all species with this type of anatomy, the xylem part of the peripheral VBs is facing towards the outside of the leaf while the phloem part is facing towards the interior water

storage tissue. Water storage cells contain some chloroplasts, including those adjacent to BS cells of peripheral VBs (not shown). All three species have grana-deficient chloroplasts in BS cells in the centripetal position (Fig. 2J, K, N, O), while M chloroplasts have prominent grana (Fig. 2L, P; and *P. pilosa*, not shown).

In *P.* cf. *bicolor*, VBs are completely surrounded by BS cells, but elongated M cells are more developed on the adaxial sides of the VBs (Fig. 2Q). BS cells have centripetal positioning of organelles (Fig. 2R) and grana-deficient chloroplasts (practically agranal, Fig. 2S) with an intensively developed system of convoluted thylakoids forming a system similar to a peripheral reticulum, but in the middle part of the chloroplast (Fig. 2S), while M chloroplasts have well-developed grana (Fig. 2T). Chloroplasts in the BS cells located on the abaxial side of the VBs are less abundant and much smaller, and they have a higher degree of development of small grana (consisting of many paired thylakoids, or grana having 3–7 thylakoids; not shown) in comparison with chloroplasts in BS cells on the adaxial side. In this species, there is an additional layer of enlarged M-like cells on the abaxial side of VBs, containing a few chloroplasts that are filled with starch, and having a well-developed system of grana (not shown). The general pattern of organelle distribution in palisade M and in BS cells is similar to that in the previous group (*P. amilis*, *P. grandiflora*, and *P. pilosa*).

A light microscopy study of leaf cross-sections of *P. cryptopetala* further illustrates a dorsoventral-type anatomy with two layers of palisade parenchyma on the adaxial side and three layers of loosely arranged, spongy parenchyma cells on the abaxial side; the middle part of the blade has rather closely arranged VBs surrounded by large BS cells with 2–3 layers of large parenchyma cells between them (Fig. 2U). A significant number of BS organelles are located in the centripetal position, adjacent to VBs, or along the radial cell walls (Fig. 2V). Closer examination of the BS cell structure in comparison with M cells shows that they contain numerous chloroplasts and enlarged mitochondria (Fig. 2W). Both M and BS chloroplasts have a well-developed system of grana (Fig. 2W, X).

Western blot analysis

Immunoblots for the main photosynthetic enzymes, PEPC, PPDK, NAD-ME, NADP-ME, PEP-CK, and Rubisco, from total soluble proteins extracted from leaves of the *Portulaca* species studied, are presented in Fig. 3. The carboxylase of the C_3 pathway, Rubisco, analysed by western blot with large subunit antibody, is abundant in all species. *Portulaca amilis*, *P.* cf. *bicolor*, *P. grandiflora*, *P. molokiniensis*, *P. oleracea*, *P. pilosa*, and *P. umbraticola* have significant labelling of the C_4 pathway enzymes, PEPC and PPDK. With respect to C_4 decarboxylases, *P. oleracea* and *P. molokiniensis* have clear labelling for NAD-ME and no labelling for NADP-ME, while the other species listed above have clear bands for NADP-ME, and only light labelling for NAD-ME. There were no immunoreactive bands for the decarboxylase PEP-CK in the *Portulaca* species, whereas in the control PEP-CK-type species *S. anglica* (see Voznesenskaya *et al.*, 2006) there is a strong immunoreactive band. In *P. cryptopetala*, there is much lower labelling for PEPC than in other species, very low intensity labelling for PPDK and NAD-ME, and no labeling for other decarboxylases. The labelling pattern in *P. cryptopetala* is similar to that of *S. portulacastrum* (Aizoaceae), a representative C_3 species (Lüttge *et al.*, 1989; Lokhande *et al.*, 2009).

Carbon isotope composition and gas exchange measurements

The *Portulaca* species in this study having Kranz-type leaf anatomy have C_4-type $\delta^{13}C$ values (–12.0 to –15.4), while *P. cryptopetala* exhibits C_3-type values (mean –30.5‰). The C_3 species *S. portulacastrum*, which has succulent flattened leaves, has a $\delta^{13}C$ of –29.5‰ (Table 1).

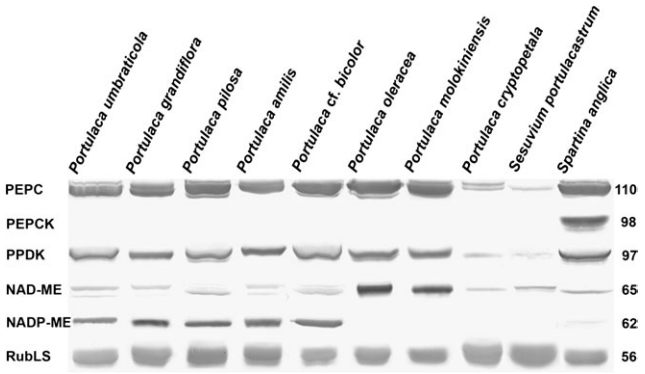

Fig. 3. Western blots for C_4 enzymes and Rubisco from total soluble proteins extracted from leaves of eight *Portulaca* species, the C_3 species *Sesuvium portulacastrum,* and the C_4 PEP-CK species *Spartina anglica*. Blots were probed with antibodies raised against PEPC, PPDK, NAD-ME, NADP-ME, PEP-CK, and Rubisco, respectively. Numbers on the left indicate molecular mass in kilodaltons. Subtle differences in blot intensity might occur due to differences in antigenicity between species.

Table 1. *CO_2 compensation points (Γ and Γ^*) and carbon isotope ratios ($\delta^{13}C$) for* Portulaca *species and* Sesuvium portulacastrum

Means are from 2–4 individual measurements ±SE.

Species	Γ (μbar)	Γ^*(μbar)	$\delta^{13}C$ (‰)
Portulaca amilis	ND	ND	–13.4±0.03
P. cf. *bicolor*	ND	ND	–15.4±0.001
P. cryptopetala	24.8±1.2	19.4±1.4	–30.5±0.21
P. grandiflora	ND	ND	–12.0±0.57
P. molokiniensis	ND	ND	–15.3±0.37
P. oleracea	3.8 ±0.6	2.0 ±0.4	–13.9±0.83
P. pilosa	ND	ND	–14.0±0.25
P. umbraticola	ND	ND	–13.4±0.29
Sesuvium portulacastrum	42.9 ±0.9	37.2 ±1.4	–29.5±0.07

ND, not determined.

Since *P. cryptopetala* does not have C_4-type $\delta^{13}C$ values, and it lacks Kranz anatomy and C_4-type enzyme composition, gas exchange analysis was made comparing this species with the C_4 species *P. oleracea* and the C_3 species *S. portulacastrum*. The Γ values, measured at 25 °C and a PPFD of 900 μmol quanta m^{-2} s^{-1}, were 3.8 μbar for *P. oleracea* and 42.9 μbar for *S. portulacastrum*, while values in *P. cryptopetala* were intermediate, 24.8 μbar (Table 1). Γ* values, measured from analysis of the intercept of CO_2 response curves at different light intensities, which corrects for the effect of dark type respiration on Γ, were 37.2 μbar for *S. portulacastrum* and 19.4 μbar for *P. cryptopetala.*

The response curves for CO_2 fixation were measured at varying intercellular levels of CO_2 under atmospheric O_2 (21%). The C_4 species *P. oleracea* shows a rapid increase in photosynthesis under increasing intercellular CO_2, with near saturation at ~400 μbar CO_2, whereas *P. cryptopetala* and *S. portulacastrum* had a C_3-like response, with photosynthesis not being fully saturated up to 1300 μbar CO_2 (Fig. 4).

Immunolabelling for GDC

In situ immunolabelling for GDC was examined in *P. cryptopetala*, *P. oleracea*, and the C_3 species *S. portulacastrum.* Analysis of the immunolabelling distribution for anti-GDC antibody at the electron microscopy level shows that in the C_4 species *P. oleracea*, gold particles are selectively localized in BS mitochondria (Fig. 5A); labelling in M mitochondria is very low, near background levels (Fig. 5B; see also the graph showing the density of gold particles per BS and M mitochondria in Fig. 5C). Similarly, in *P. cryptopetala* there is clear selective labelling for GDC in BS mitochondria (Fig. 5D–F). In comparison, in the C_3 species *S. portulacastrum*, there is equivalent labelling of GDC in mitochondria of M and BS cells (Fig. 5G–I).

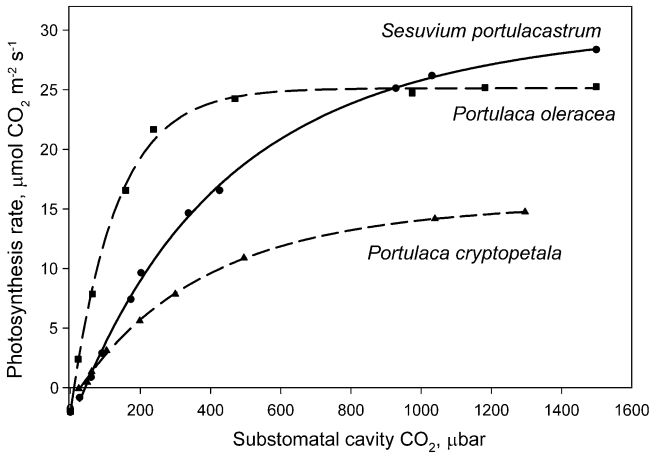

Fig. 4. Rates of CO_2 fixation in response to varying intercellular levels of CO_2 at 21% O_2, 25 °C, and a PPFD of 900 μmol quanta m^{-2} s^{-1} in *Portulaca cryptopetala*, *P. oleracea*, and *Sesuvium portulacastrum*. The results represent the average from measurements of the response to changes in CO_2 (from ambient to low, and low to high) from separate measurements on 2–3 leaves from different plants.

Analysis of stomata on leaves

Among the species studied, stomata were found to be present on the adaxial side and totally absent on the abaxial side of the leaf of *P.* cf. *bicolor* (epistomatic type, Fig. 6I, J). All other species have stomata on both sides of the leaf, indicative of amphistomatic type (Fig. 6A–H, K, L). The stomata in all species are of the paracytic type with two subsidiary cells, and they have an irregular orientation in relation to the axis of the leaf in all species having broad leaves (*P. umbraticola*, *P. oleracea*, *P. amilis*, *P.* cf. *bicolor*, *P. cryptopetala*, and *P. molokiniensis*), while they are mostly perpendicular to the leaf main vein in species with cylindrical leaves (*P. grandiflora* and *P. pilosa*).

Analysis of chlorophyll content

The leaf chlorophyll content was measured per fresh and dry weight and per area exposed to incident light (Table 2). In leaves there is large variation in chlorophyll content calculated on a fresh weight (FW) basis, ranging from 0.21 μg mg FW^{-1} up to 0.73 μg mg FW^{-1} across the eight *Portulaca* species, with the lowest values in *P. grandiflora* and *P. pilosa* which have succulent terete leaves. On a dry weight (DW) basis the species which have the lowest chlorophyll content (ranging from 17 μg mg DW^{-1} to 20 μg mg DW^{-1}) have VBs distributed more or less in one paradermal plane (*P.* cf. *bicolor*, *P. oleracea*, *P. umbraticola*, and *P. molokiniensis*), while species having high chlorophyll content (23, 27, and 37 μg mg DW^{-1} for *P. pilosa*, *P. amilis*, and *P. grandiflora*, respectively) have VBs distributed around the leaf periphery. On a leaf area basis the C_3–C_4 intermediate *P. cryptopetala* had the highest chlorophyll content, while values ranged from 34 μg cm^{-2} to 50 μg cm^{-2} among the C_4 *Portulaca* species. The chlorophyll content in the C_3 species *S. portulacastrum* on a weight and area basis is similar to that of the C_3–C_4 intermediate *P. cryptopetala*, both lacking Kranz anatomy.

Analysis of cotyledons

There is vast variation in the distribution of VBs in leaves of the *Portulaca* species studied with Kranz-type chlorenchyma; however, the cotyledons, except for *P.* cf. *bicolor*, all have Atriplicoid-like anatomy with VBs distributed in one lateral plane (Fig. 7, left column, not shown for *P. molokiniensis* and *P. pilosa*). In most of the species studied, the VBs are surrounded by two layers of chlorenchyma cells, with mostly one layer of colourless hypodermal cells on the abaxial side of the cotyledon (Fig. 7A, D, G, J), except for *P. umbraticola*, which has hypodermal layers on both sides of the cotyledon (Fig. 7A). In *P.* cf. *bicolor*, cotyledons (Fig. 7M) have the same structure as leaves (Fig. 2Q): the VBs are located adjacent to the adaxial epidermis of the cotyledon, with reduced development of Kranz on the lower side of the VBs, and there are two layers of colourless hypodermal cells on the abaxial side.

Cotyledons of *P. cryptopetala* have C_3-like anatomy, with one layer of palisade-like M cells on the adaxial side and

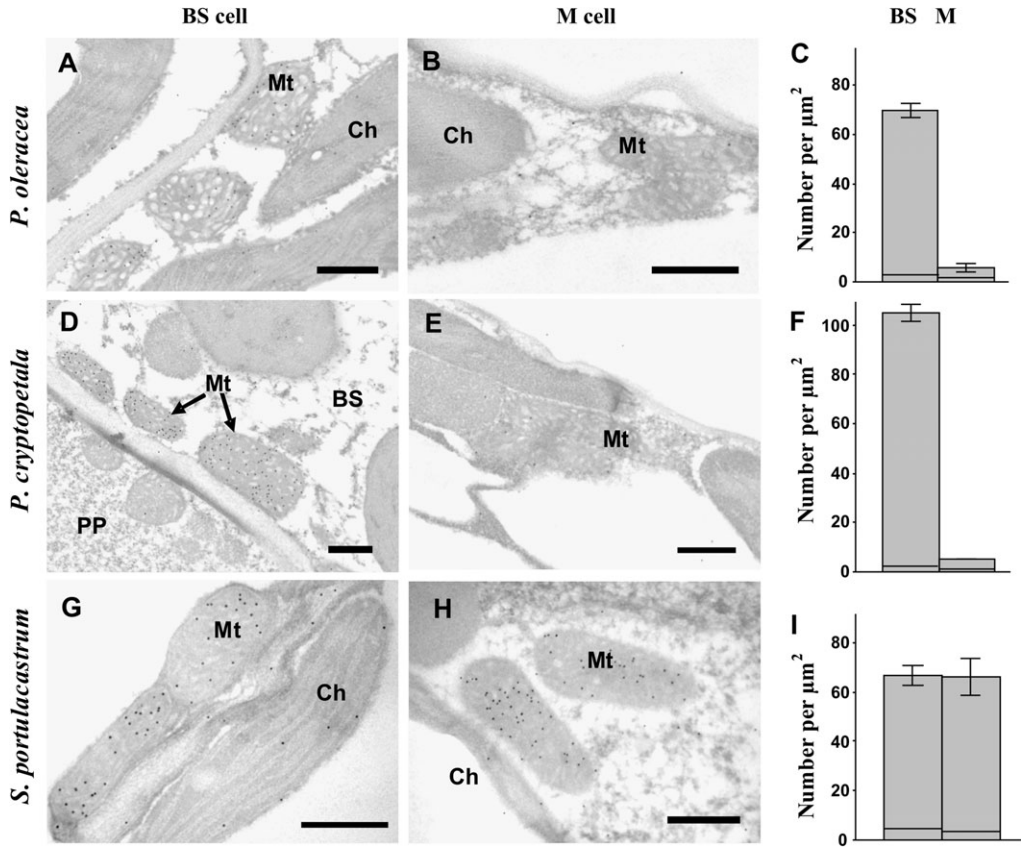

Fig. 5. Electron microscopy of *in situ* immunolocalization of glycine decarboxylase (GDC) in chlorenchyma cells of *P. oleracea* (A, B), *P. cryptopetala* (D, E), and *Sesuvium portulacastrum* (G, H), and graphs showing the density of labelling for GDC in BS versus M mitochondria (right panels C, F, and I). (A, D, G) Immunolabelling of GDC in bundle sheath cell mitochondria. (B, E) Lack of immunolabelling for GDC in M cells of two *Portulaca* species, and (H) showing the presence of gold particles in M mitochondria in *S. portulacastrum*. (C, F, I) In all graphs the *x*-axis represents the number of gold particles per μm^2 of mitochondrial area; for each cell type 10–60 cell fragments were used for counting. The horizontal lines near the base of the bars represent the level of background (number of particles per cell fragment area excluding mitochondria). BS, bundle sheath cell; Ch, chloroplast; M, mesophyll; Mt, mitochondria; PP, phloem parenchyma cell. Scale bars: 0.5 µm.

two layers of spongy M cells on the abaxial side (Fig. 7P). VBs are surrounded by enlarged BS cells, with organelles mostly in a centripetal position (Fig. 7P); there are numerous chloroplasts and mitochondria in the centripetal position or along the radial cell walls, similar to that described for leaves (analysis by transnission electron microscopy, not shown).

Analysis of stems

Young stems of *Portulaca* species have a rather thick primary cortex consisting of 6–10 layers of parenchyma cells (Fig. 7, middle column). There is a subepidermal layer of tightly arranged cells with thickened cell walls in all species, but the level of thickening differs between species: in *P. amilis*, hypodermal cells have a higher level of thickening especially in the corners towards the airspaces (Fig. 7K), while in *P. oleracea* the thickening is not very pronounced (Fig. 7E). No signs of Kranz-type anatomy were found; chlorenchyma cells in stems of all species exhibit C_3-type structure. All species have some chloroplasts in cortex cells, with increasing occurrence towards the central cylinder (observed under the fluorescent microscope, not shown). Young stems of *P.* cf. *bicolor* are brown, while in other species they are light or reddish-green. The chlorophyll content of stems, versus that in leaves, was determined on an area (two-dimensional, e.g. an area exposed to incident light), FW, and DW basis (Table 2). On an FW and DW basis the stems of the *Portulaca* species had on average about one-third as much chlorophyll as leaves. On an incident area basis the chlorophyll content of stems across species ranged from 30% to 60% of that of leaves, while there was more variation between species on a weight basis.

The epidermis of the stem of *P. cryptopetala* has numerous stomata (Fig. 7R) which are oriented along the stem axis, while in all other species there are practically no stomata on stems or only an occasional single stomate was observed (Fig. 7C, F, I, L, O).

Discussion

This study reports on structural and biochemical forms of photosynthesis in *Portulaca* species using representatives

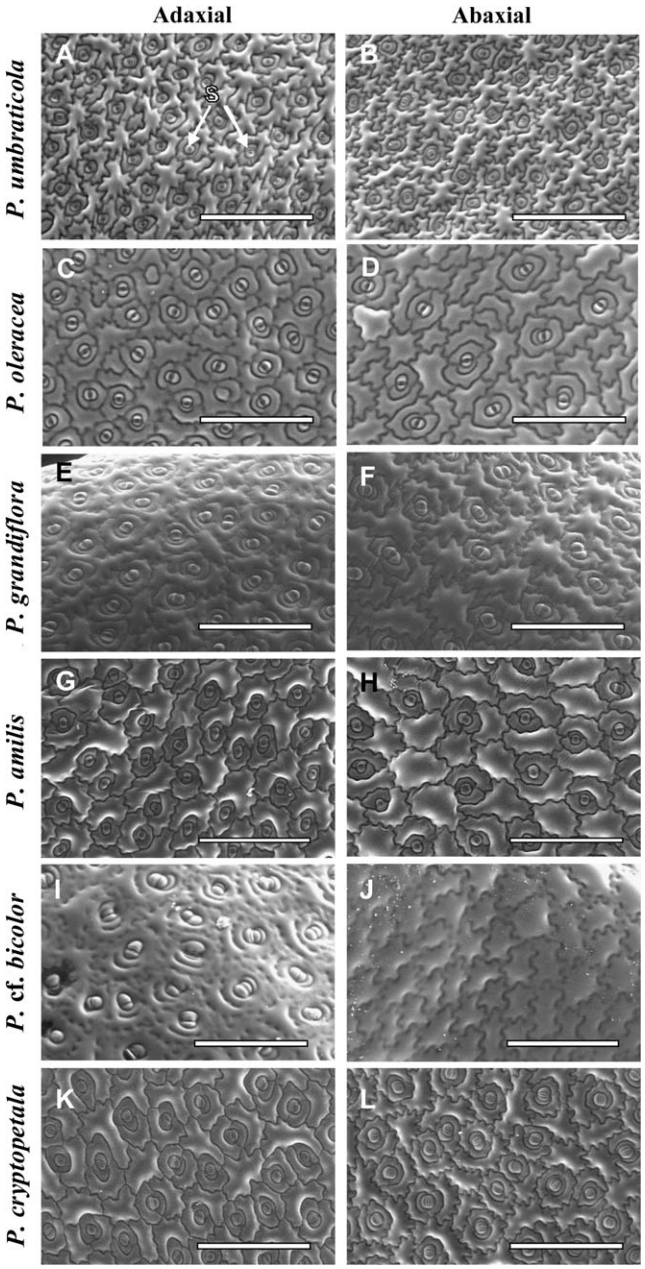

Fig. 6. Scanning electron micrographs showing stomata distribution on the adaxial (A, C, E, G, I, K) and abaxial (B, D, F, H, J, L) leaf surfaces in six *Portulaca* species: *P. umbraticola* (A, B), *P. oleracea* (C, D), *P. grandiflora* (E, F), *P. amilis* (G, H), *P.* cf. *bicolor* (I, J), and *P. cryptopetala* (K, L). S, stomata. Scale bars: 400 μm.

of the major lineages known in the genus. The genus contains ~100 species distributed around the world, and the most recent and accepted infrageneric classification was proposed by Geesink (1969). This author subdivided *Portulaca* into two subgenera, *Portulacella* (containing species with glabrous nodes and flowers in open dichasia) and *Portulaca* (species mostly with axillary or nodal scales and/or hairs and flowers in sessile terminal clusters or solitary, surrounded by a whorl of leaf-like bracts). Recent phylogenetic analysis of molecular data has revealed the presence of two well-defined clades within *Portulaca* (G Ocampo and JT Columbus, unpublished results) which roughly corresponds to the infrageneric classification proposed by Geesink (1969). However, in order to maintain monophyletic groups, changes to Geesink's classification will be made at the subgeneric and sectional levels in which subgenus *Portulaca,]* will include species with alternate leaves, while subgenus *Portulacella* will embrace taxa with opposite leaves. Furthermore, in subgenus *Portulaca* there are three subclades, Oleracea, Pilosa, and Umbraticola (G Ocampo and JT Columbus, unpublished results).

From subgenus *Portulaca, P. umbraticola* was studied in the Umbraticola clade; *P. oleracea*, *P. molokiniensis*, and *P. cryptopetala* in the Oleracea clade (the latter species found to be a C_3–C_4 intermediate); and *P. grandiflora*, *P. pilosa*, and *P. amilis* in the Pilosa clade. *Portulaca* cf. *bicolor* is a representative from subgenus *Portulacella*. All species are endemic to the New World, except for *P.* cf. *bicolor* which is an Australian taxon, and *P. oleracea* which is widely distributed around the world as a weed, but its origin is unknown.

In the genus there is large variation among species in leaf morphology, leaf types, from flattened to semi-terete to terete leaves, with differences in thickness and degree of succulence, and in chlorophyll content. The species examined having more succulent leaves have lower chlorophyll content on an FW basis (e.g. *P. molokiniensis*, *P. grandiflora*, and *P. pilosa*). On a DW basis Atriplicoid-type species with flattened leaves have a lower chlorophyll content than semi-terete/terete leaves, which may reflect differences in light interception and arrangement of the Kranz tissue.

Types of photosynthesis in leaves

From analysis of leaf structure, and C_4 cycle biochemical subtypes, in a few representative species from four lineages in genus *Portulaca*, four forms of C_4 were identified. Also, a C_3–C_4 intermediate *Portulaca* species was discovered in the genus. Following is a summary of some key features of these photosynthetic types.

Portulaca umbraticola*, Atriplicoid Kranz anatomy, NADP-ME-type:* This species is a member of the Umbraticola clade (subgenus *Portulaca*). It has flattened amphistomatic leaves with a 'classical' Atriplicoid type of leaf anatomy which is widely distributed among C_4 dicot species. It has lateral distribution of veins surrounded by dual concentric rings of chlorenchyma; the hypoderm, when present, usually fulfils the role of water storage tissue (McKown *et al.*, 2005; Muhaidat *et al.*, 2007). It is classified as an NADP-ME-type C_4 species based on western blots for C_4 decarboxylases and deficiency of grana in BS chloroplasts. NADP-ME-type C_4 species are well known to have reduced grana and less photosystem II-dependent linear electron flow for production of NADPH, since they have predominantly a malate-type C_4 shuttle which donates both CO_2 and reductive power to BS chloroplasts (Edwards and Walker 1983).

Portulaca oleracea *and* P. molokiniensis*, Atriplicoid Kranz anatomy, NAD-ME-type:* Species in the Oleracea clade (subgenus *Portulaca*) have a variant of Atriplicoid type anatomy characterized by the lateral VBs distributed unevenly in the

Table 2. *Chlorophyll content in mature leaves and young stems of* Portulaca *species and* Sesuvium portulacastrum.
Means are from 4–6 individual measurements ±SE. Lower case letters indicate significant differences between species in each column, at P <0.05.

Species	Chl *a+b* (μg mg FW^{-1})		Chl *a+b* (μg mg DW^{-1})		Chl *a+b* (μg cm^{-2})	
	Leaf	Stem	Leaf	Stem	Leaf	Stem
P. amilis	0.51 ± 0.04^{bc}	0.19 ± 0.01^{c}	26.9 ± 1.3^{bc}	5.6 ± 0.1^{ab}	48.4 ± 5.3^{bc}	29.9 ± 3.0^{bc}
P. cf *bicolor*	0.45 ± 0.04^{b}	0.48 ± 0.03^{d}	17.1 ± 1.9^{a}	8.5 ± 1.4^{b}	50.3 ± 1.6^{bc}	26.9 ± 1.5^{bc}
P. cryptopetala	0.72 ± 0.06^{d}	0.15 ± 0.01^{c}	20.0 ± 2.0^{a}	4.7 ± 0.6^{ab}	61.2 ± 4.0^{c}	30.5 ± 3.9^{c}
P. grandiflora	0.31 ± 0.01^{a}	0.07 ± 0.005^{a}	36.8 ± 5.2^{c}	5.0 ± 1.5^{ab}	38.1 ± 1.9^{b}	11.8 ± 1.1^{a}
P. molokiniensis	0.21 ± 0.02^{a}	ND	19.4 ± 2.8^{a}	ND	18.0 ± 1.6^{a}	ND
P. oleracea	0.73 ± 0.04^{d}	0.17 ± 0.03^{c}	19.9 ± 2.1^{a}	3.0 ± 0.3^{a}	35.6 ± 2.6^{b}	19.0 ± 3.4^{ab}
P. pilosa	0.41 ± 0.02^{ab}	0.14 ± 0.01^{bc}	22.6 ± 2.1^{ab}	2.9 ± 0.3^{a}	33.7 ± 1.6^{b}	13.0 ± 1.2^{a}
P. umbraticola	0.51 ± 0.04^{bc}	0.08 ± 0.01^{a}	18.4 ± 1.2^{a}	2.3 ± 0.1^{a}	35.0 ± 2.4^{b}	14.8 ± 2.9^{a}
Average for *Portulaca* species	0.52	0.18	23.1	4.6	43.2	20.8
S. portulacastrum	0.64 ± 0.07^{cd}	0.09 ± 0.01^{ab}	16.0 ± 0.8^{a}	2.0 ± 0.06^{a}	64.6 ± 9.2^{c}	14.3 ± 1.0^{a}

paradermal plane, with the lower order VBs situated closer to the abaxial side. In addition to *P. molokiniensis*, this zig-zag pattern of distribution can also be seen in the Hawaiian species, *P. lutea* (Kim and Fisher, 1990).

As noted in the Introduction, *P. oleracea* is a well-known example of a dicot species with NAD-ME-type biochemistry with ultrastructural features characteristic for this type: numerous mitochondria, and chloroplasts with well-developed grana, in BS cells and grana-deficient chloroplasts in M cells (Downton, 1971; Gutierrez *et al.*, 1974; Kim and Fisher, 1990). It was the only species in the genus known to have NAD-ME-type C_4 photosynthesis. However, similar ultrastructural features for BS and M cells (with numerous mitochondria and chloroplasts having well-developed grana in BS and grana-deficient chloroplasts in M) were found in *P. lutea* Sol. ex G. Forster and *P. molokiniensis* Hobdy (Kim and Fisher, 1990; this study), which are also members of the Oleracea clade (G Ocampo and JT Columbus, unpublished results), suggesting that these two species are also NAD-ME-type C_4. This assumption was confirmed in the present study for *P. molokiniensis* by western blot analysis. The well-developed grana in BS chloroplasts support photosystem II-dependent linear electron flow for production of NADPH that is utilized in the C_3 cycle. This is characteristic of this subtype, where aspartate is a major donor of CO_2 to BS cells in which the C_4 shuttle transfers CO_2, but not reductive power, from the M to BS cells. It is also interesting that these three species have a similar Atriplicoid leaf anatomy in which the VBs have a zig-zag distribution pattern.

Portulaca grandiflora*,* P. pilosa *and* P. amilis*, Pilosoid Kranz anatomy, NADP-ME-type:* These species are members of the Pilosa clade (subgenus Portulaca). *Portulaca amilis* has flattened obovate or spatulate leaves while *P. grandiflora* and *P. pilosa* have subterete to terete leaves. The lateral VBs with Kranz anatomy are distributed around the leaf periphery; the main vein, which lacks a chlorenchyma sheath, is enclosed by water storage tissue located in the central part of the leaf (see also the anatomy of *P. grandiflora* in Nishioka *et al.*, 1996). This form of leaf anatomy was also shown in the Hawaiian species *P. villosa* Cham., *P. sclerocarpa* A. Gray, and *P. 'ulupalakua'* by Kim and Fisher (1990). This type of Kranz, with peripheral distribution of VBs, is designated here as Pilosoid according to the clade Pilosa with two variants: more rounded leaves (e.g. *P. grandiflora*) versus flattened leaves (as in *P. amilis*). Additional variations in anatomy include the obvious absence of hypodermal cell layers in *P. amilis* and *P. pilosa*, while there is a clearly distinguished hypodermal layer in *P. grandiflora* (current study) and in the Hawaiian species *P. sclerocarpa* (Kim and Fisher, 1990). As noted in the Introduction, *P. grandiflora* was earlier characterized as an NADP-ME-type C_4 species, which is confirmed in the present study, along with evidence that *P. pilosa* and *P. amilis* belong to this biochemical subtype which has granal deficiency in BS chloroplasts. Ultrastructural features of chlorenchyma cells of the three Hawaiian species, *P. villosa*, *P. sclerocarpa*, and *P. 'ulupalakua'* (Kim and Fisher, 1990), suggest that these are also NADP-ME-type C_4 plants. Also, molecular phylogenetic analyses on *P. villosa* and *P. sclerocarpa* show that they are members of the Pilosa clade (G Ocampo and JT Columbus, unpublished results).

Portulaca cf. bicolor*, Portulacelloid Kranz anatomy, NADP-ME-type:* This species of subgenus *Portulacella* has an interesting leaf anatomy, in which Kranz-type chlorenchyma cells surround the VBs towards the adaxial side of the leaf, while there is underlying water storage tissue towards the abaxial side. This type of leaf anatomy was previously reported in *P. oligosperma* F. Muell. (Carolin *et al.*, 1978), *P. quadrifida* L., and *P. wightiana* Wall. ex Wight & Arn. (Prabhakar and Ramayya, 1979) which also occurs in subgenus *Portulacella* (*sensu* G Ocampo and JT Columbus, unpublished results). This form of Kranz is designated Portulacelloid according to the subgenus name. It resembles somewhat the Kochioid type of leaf anatomy in Chenopodiaceae (Carolin *et al.*, 1975; Edwards and Voznesenskaya, 2010), which has arcs of chlorenchyma above the peripherally arranged VBs. However, in the Kochioid type, M and BS cells are arranged only on the adaxial side of the VBs. In *P.* cf. *bicolor*, BS cells completely enclose VBs, but

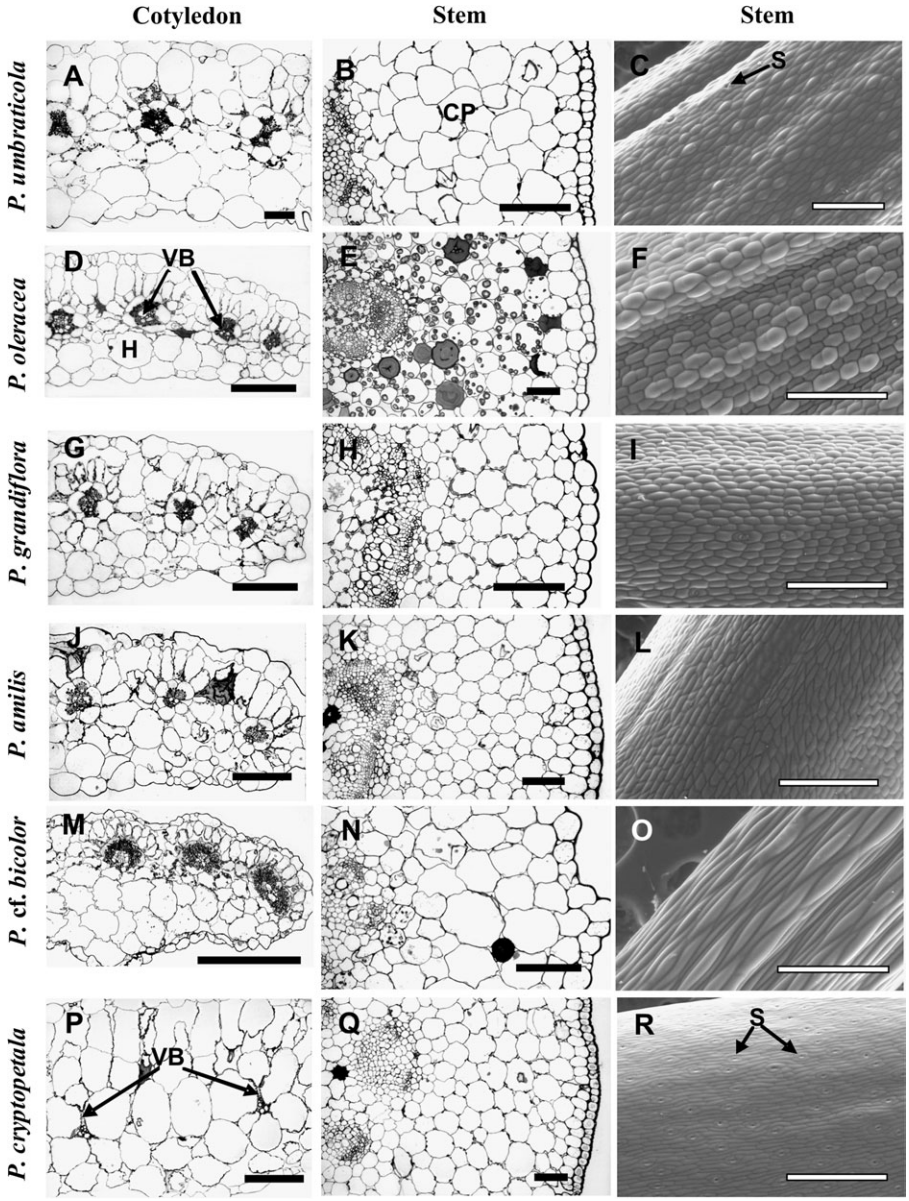

Fig. 7. Light micrographs showing cross-sections of cotyledons (A, D, G, J, M, P) and young stems (B, E, H, K, N, Q), and scanning electron microscopy of stem epidermis (C, F, I, L, O, R) for six *Portulaca* species: *P. umbraticola* (A–C), *P. oleracea* (D–F), *P. grandiflora* (G–I), *P. amilis* (J–L), *P.* cf. *bicolor* (M–O), and *P. cryptopetala* (P–R). CP, cortex parenchyma; H, hypoderm; VB, vascular bundle. Scale bars: 200 μm for cotyledons (left column); 100 μm for stem cross-sections (middle column); 500 μm for C, F, I, L, R, and 400 μm for O for stem epidermis (right column).

the BS cells on the abaxial side of the VBs contain fewer organelles and the chloroplasts have more grana compared with those in BS cells on the adaxial side. Palisade M cells are located on the adaxial and lateral sides of the VBs, and there are enlarged M cells on the abaxial side of the VBs, which have chloroplasts with large starch grains. However, there were no M cells reported on the abaxial side of the VBs for *P. quadrifida* or *P. wightiana* by Prabhakar and Ramayya (1979). *Portulaca* cf. *bicolor* is an NADP-ME-type C_4 species based on analysis by western blots and the reduced grana formation in the BS chloroplasts.

Portulaca cf. *bicolor* is the only species in this study which has epistomatic type leaf; however, *P. quadrifida* (Ramayya and Rajagopal, 1974) and *P. oligosperma* (Ogburn and Edwards, 2009) in subgenus *Portulacella* have also been reported to have epistomatic leaves. This is consistent with a large volume of water storage tissue on the abaxial side of the leaf, which creates a longer diffusion path for CO_2 from the atmosphere to the chlorenchyma tissue than in the other structural types of *Portulaca*.

Portulaca cryptopetala*, C_3–C_4 intermediate with C_3 like dorsoventral anatomy:* This species in the Oleracea clade lacks Kranz anatomy and it was identified as a C_3–C_4 intermediate based on CO_2 compensation point, arrangement of organelles in BS cells, and immunolocalization of GDC. From analysis by gas exchange, Γ* of *P. cryptopetala*

was 19.4 μbar. In comparison, the C_3 species *S. portulacastrum* had a Γ* value of 37.2 μbar, which is close to the predicted value for C_3 species at 25 °C (Furbank *et al.*, 2009), while *P. oleracea* has a C_4 type Γ* of 2.0 μbar. C_4 species typically have Γ values between 0 μbar and 5 μbar, and C_3–C_4 intermediates between 9 μbar and 30 μbar depending on the species (e.g. Ku *et al.*, 1991; Vogan *et al.*, 2007).

Microscopy studies on *P. cryptopetala* show that BS cells have chloroplasts and enlarged mitochondria uniquely located towards a centripetal position, which is consistent with it being identified as a C_3–C_4 intermediate. Also, in *P. cryptopetala* GDC is selectively localized in mitochondria of BS cells which is considered an important test to distinguish between C_3 and C_3–C_4 intermediate forms of photosynthesis (Rawsthorne *et al.*, 1988). In C_3–C_4 intermediates, and in C_4 species (*P. oleracea* in this study) GDC is localized only in mitochondria of BS cells, while in C_3 species (*S. portulacastrum* in this study) GDC is present in mitochondria of M and BS cells.

Western blots of C_4 pathway enzymes showed that PEPC and PPDK were both detectable in *P. cryptopetala*, but at much lower levels than in the C_4 species. Thus, there may be little or no function of a C_4 cycle in this species, as it has a C_3-type carbon isotope value (–30.5‰). This type of intermediate (called Type I) can have an increase in their efficiency of photosynthesis when CO_2 is limiting by refixing photorespired CO_2 in BS cells, rather than by utilizing a C_4 cycle (Edwards and Ku, 1987; Ku *et al.*, 1991; Rawsthorne and Bauwe, 1998). *Portulaca cryptopetala* is widely distributed in the central part of South America where it is usually associated with moist, warm habitats. This species might be an ancestor to C_4 species which evolved in clade Oleracea, enabling them (e.g. *P. oleracea*) to be more tolerant to dryer habitats where CO_2 is more limiting due to lower stomatal conductance.

Types of anatomy in cotyledons

All *Portulaca* species examined having Kranz-type anatomy in leaves, also have Kranz anatomy in the cotyledons. In *P.* cf. *bicolor* the type of Kranz anatomy in cotyledons is the same as in leaves, which is named Portulacelloid type. In the other C_4 species, *P. umbraticola*, *P. oleracea*, *P. molokiniensis*, *P. amilis*, and *P. grandiflora*, there is diversity in the forms of Kranz anatomy in leaves while they all have cotyledons with Atriplicoid-type anatomy with the VBs in one paradermal plane and prominent hypodermal cells mostly on the abaxial side in all species except for *P. umbraticola*, which has hypodermal layers on both sides of the cotyledon. In other studies on C_4 dicots, the anatomy and type of photosynthesis in cotyledons has often been found to be similar to that in leaves; but differences have been observed in studies of C_4 in family Chenopodiaceae. In some C_4 chenopods, the cotyledons have the same C_4 biochemical subtype as in leaves, but a more primitive type of anatomy; for example, *Kochia scoparia* has Atriplicoid-type anatomy in cotyledons versus Kochioid-type anatomy in leaves, and *Salsola laricina* has Atriplicoid-type anatomy in cotyledons versus Salsoloid-type anatomy in leaves (Pyankov *et al.*, 1999*a*, 2000). Also, *Salsola gemmascens*, *Haloxylon* spp., and *Halocharis gossypina* have Kranz anatomy and C_4 photosynthesis in leaves, while their cotyledons have C_3 type of anatomy and biochemistry (Pyankov *et al.*, 1999*b*, 2000; Voznesenskaya *et al.*, 1999).

In *P. cryptopetala*, the cotyledons have C_3-type dorsoventral anatomy with a high concentration of organelles in BS cells in the centripetal position, similar to that of leaves, which is a characteristic of C_3–C_4 intermediate type of photosynthesis (Edwards and Ku, 1987; Rawsthorne and Bauwe, 1998).

Structural features of stems

The general anatomy of stems was examined to determine the occurrence of chloroplasts and types of structure of the primary cortex. Among the species of *Portulaca*, the stem anatomy was very similar, with multiple layers of cortical parenchyma cells. The density of chloroplasts was a little higher in the more internal cortical cells; these parenchyma cells are C_3 like, with no signs of Kranz-type anatomy. The stems of all species have significant levels of chlorophyll (e.g. on average about half that of leaves on an incident area basis) which suggests ability to contribute to carbon assimilation.

The C_3–C_4 intermediate species, *P. cryptopetala*, has numerous stomata on the epidermis of stems, indicating potential for gas exchange with the atmosphere, with chlorophyll content ~50% of that of leaves on an area basis. In all of the C_4 *Portulaca* species in this study, few to no stomata were observed on stems; Ogburn and Edwards (2009) also reported low numbers of stem stomata in samples of *P. amilis* and *P. pilosa*. The layer of cells beneath the epidermis of the stem in all species shows collenchyma-like thickening of the cell wall; it was most apparent in *P. amilis*, such that there appears to be little intercellular air space. This cell wall thickening combined with few to no stomata on the stem epidermis of the C_4 species may provide high resistance to water loss, enabling them to remain viable even under stressful conditions. Also, in the C_4 species it suggests that any CO_2 assimilated by the chloroplasts would be derived from refixation of respired CO_2, rather than by intake of atmospheric CO_2. Two of these species, *P. oleracea* and *P. grandiflora*, are known to be induced to perform CAM under water stress (Koch and Kennedy, 1980; 1982; Guralnick *et al.*, 2002; Lara *et al.*, 2003). This could allow respired CO_2 in stems at night to be fixed into malate, with subsequent donation of CO_2 from malate to the C_3 cycle during the day. In *P. grandiflora*, there is evidence for CAM-idling in stems (which prevents loss of respired CO_2 during both the night and day); stomata were reported to be absent and the stems undergo diurnal fluctuations in acidity characteristic of CAM (Guralnick *et al.*, 2002).

In summary, this study describes the diverse forms of C_4 photosynthesis in major lineages in the genus *Portulaca*,

along with comparative structural analyses of cotyledons and stems. C_4 photosynthesis is advantageous in climates where CO_2 tends to be limiting, which can occur under high temperatures, and in habitats with water deficits which cause reduced stomatal conductance. In semi-arid regions, there are C_4 plants having semi-terete/terete leaves with water storage tissue; for example, in clade Pilosa in genus *Portulaca* and in some succulent subfamilies in Chenopodiaceae (Eggli, 2002; Edwards and Voznesenskaya, 2010). Interestingly, in *Portulaca*, which is the only genus in Portulacaceae known to have C_4 species, a C_3–C_4 intermediate, *P. cryptopetala*, was identified in clade Oleracea in this study. C_3–C_4 intermediate species are of considerable interest as they may provide clues to the evolutionary transition from C_3 to C_4 photosynthesis; they have been identified in a number of families including Asteraceae, Amaranthaceae, Boraginaceae, Brassicaceae, Chenopodiaceae, Cleomaceae, Molluginaceae, Poaceae, and, in the present study, Portulacaceae (Edwards and Ku, 1987; McCown *et al.*, 2005; Vogan *et al.*, 2007; Voznesenskaya *et al.*, 2007). The discovery of a C_3–C_4 intermediate in *Portulaca* during structural and biochemical analyses of a limited number of species indicates that other C_3–C_4 intermediate species may be found in this and other genera in the family, which could provide insight into the mechanism of evolution of different structural and biochemical forms of C_4.

Acknowledgements

This material is based upon work supported by the National Science Foundation under Grants IBN-0131098 and IBN-0236959, NSF Isotope Facility Grant DBI-0116203, and partly by Russian Foundation of Basic Research Grant 08-04-00936. We are grateful to the Franceschi Microscopy and Imaging Center of Washington State University for use of their facilities and staff assistance, to R Sage for advice, and to C Cody for plant growth management. GO acknowledges support by Rancho Santa Ana Botanic Garden and the Comisión Nacional de Ciencia y Tecnología (Mexico).

References

Bender MM, Rouhani I, Vines HM, Black CC Jr. 1973. $^{13}C/^{12}C$ ratio changes in Crassulacean acid metabolism plants. *Plant Physiology* **52,** 427–430.

Brooks A, Farquhar GD. 1985. Effect of temperature on the CO_2/O_2 specificity of ribulose-1,5-bisphosphate carboxylase/oxygenase and the rate of respiration in the light. *Planta* **165,** 397–406.

Brown RH. 1999. Agronomic implications of C_4 photosynthesis. In: Sage RF, Monson RK, eds. *C_4 plant biology*. San Diego, CA: Academic Press, 473–508.

Carolin RC, Jacobs SWL, Vesk M. 1975. Leaf structure in Chenopodiaceae. *Botanische Jahrbücher für Systematik, Pflanzengeschichte und Pflanzengeographie* **95,** 226–255.

Carolin RC, Jacobs SWL, Vesk M. 1978. Kranz cells and mesophyll in the Chenopodiales. *Australian Journal of Botany* **26,** 683–698.

Downton WJS. 1971. The chloroplasts and mitochondria of bundle sheath cells in relation to C_4 photosynthesis. In: Hatch MD, Osmond CB, Slatyer RO, eds. *Photosynthesis and photorespiration*. New York, NY: Wiley-Interscience, 419–425.

Edwards GE, Ku MSB. 1987. The biochemistry of C_3–C_4 intermediates. In: Hatch MD, Boardman NK, eds. *The biochemistry of plants, Vol. 10, Photosynthesis*. New York: Academic Press, Inc., 275–325.

Edwards GE, Voznesenskaya E. 2010. C_4 photosynthesis: Kranz forms and single-cell C_4 in terrestrial plants. In: Raghavendra A, Sage RF, eds. *Photosynthesis and related CO_2 concentrating mechanisms. Advances in Photosynthesis Research*. Dordrecht, The Netherlands: Kluwer (in press).

Edwards GE, Walker DA. 1983. *C_3, C_4: mechanisms, and cellular and environmental regulation, of photosynthesis*. Oxford, UK: Blackwell Scientific Publications.

Eggli U. 2002. *Illustrated handbook of succulent plants: dicotyledons*. Berlin: Springer.

Furbank RT, Von Caemmerer S, Sheehy JE, Edwards GE. 2009. C_4 rice: a challenge for plant phenomics. *Functional Plant Biology* **36,** 845–856.

Geesink R. 1969. An account of the genus *Portulaca* in Indo-Australia and the Pacific (Portulacaceae). *Blumea* **17,** 294–298.

Guralnick LJ, Edwards GE, Ku MSB, Hockema B, Franceschi VR. 2002. Photosynthetic and anatomical characteristics in the C_4–Crassulacean acid metabolism-cycling plant, *Portulaca grandiflora*. *Functional Plant Biology* **29,** 763–773.

Guralnick LJ, Cline A, Smith M, Sage R. 2008. Evolutionary physiology: the extent of C_4 and CAM photosynthesis in the genera *Anacampseros* and *Grahamia* of the Portulacaceae. *Journal of Experimental Botany* **59,** 1735–1742.

Gutierrez M, Gracen VE, Edwards GE. 1974. Biochemical and cytological relationships in C_4 plants. *Planta* **119,** 279–300.

Hatch MD. 1987. C_4 photosynthesis: a unique blend of modified biochemistry, anatomy and ultrastructure. *Biochimica et Biophysica Acta* **895,** 81–106.

Kanai R, Edwards G. 1999. The biochemistry of C_4 photosynthesis. In: Sage RF, Monson RK, eds. *C_4 plant biology. Physiological ecology series*. San Diego: Academic Press, 49–87.

Kim I, Fisher DG. 1990. Structural aspects of the leaves of seven species of *Portulaca* growing in Hawaii. *Canadian Journal of Botany* **68,** 1803–1811.

Koch KE, Kennedy RA. 1980. Characteristics of Crassulacean acid metabolism in the succulent C_4 dicot, *Portulaca oleracea* L. *Plant Physiology* **65,** 193–197.

Koch KE, Kennedy RA. 1982. Crassulacean acid metabolism in the succulent C_4 dicot, *Portulaca oleracea* L. under natural environmental conditions. *Plant Physiology* **69,** 757–761.

Ku MSB, Edwards G, Tanner CB. 1977. Effects of light, carbon dioxide, and temperature on photosynthesis, oxygen inhibition of

photosynthesis, and transpiration in *Solanum tuberosum*. *Plant Physiology* **59,** 868–872.

Ku MSB, Wu J, Dai Z, Chu C, Edwards GE. 1991. Photosynthetic and photorespiratory characteristics of *Flaveria* species. *Plant Physiology* **96,** 518–528.

Laetsch WM. 1971. Chloroplast structural relationships in leaves of C_4 plants. In: Hatch MD, Osmond CB, Slatyer RO, eds. *Photosynthesis and photorespiration*. New York: Wiley-Interscience, 323–349.

Laetsch WM. 1974. The C_4 syndrome: a structural analysis. *Annual Review of Plant Physiology* **25,** 27–52.

Laisk A, Edwards GE. 1997. CO_2 and temperature-dependent induction in C_4 photosynthesis: an approach to the hierarchy of rate-limiting processes. *Australian Journal of Plant Physiology* **24,** 505–516.

Lara MV, Disante KB, Podesta FE, Andreo CS, Drincovich MF. 2003. Induction of a Crassulacean acid like metabolism in the C_4 succulent plant, *Portulaca oleracea* L.: physiological and morphological changes are accompanied by specific modifications in phosphoenolpyruvate carboxylase. *Photosynthesis Research* **77,** 241–254.

Legrand D. 1958. Desmembración del género *Portulaca* II. *Comunicaciones Botánicas del Museo de Historia Natural de Montevideo* **3,** 1–17.

Lokhande VH, Nikam TD, Suprasanna P. 2009. *Sesuvium portulacastrum* (L.) L. a promising halophyte: cultivation, utilization and distribution in India. *Genetic Resources Crop Evolution* **56,** 741–747.

Long JJ, Berry JO. 1996. Tissue-specific and light-mediated expression of the C_4 photosynthetic NAD-dependent malic enzyme of amaranth mitochondria. *Plant Physiology* **112,** 473–482.

Lüttge U, Popp M, Medina E, Cram W, Diaz M, Griffiths H, Lee H, Schafer C, Smitch J, Stimmel K- H. 1989. Ecophysiology of xerophytic and halophytic vegetation of a coastal alluvial plain in northern Venezuela. V. The *Batis maritima–Sesuvium portulacastrum* vegetation unit. *New Phytologist* **111,** 283–291.

Maurino VG, Drincovich MF, Andreo CS. 1996. NADP-malic enzyme isoforms in maize leaves. *Biochemistry and Molecular Biology International* **38,** 239–250.

McKown AD, Moncalvo J-M, Dengler NG. 2005. Phylogeny of *Flaveria* (Asteraceae) and inference of C_4 photosynthesis evolution. *American Journal of Botany* **92,** 1911–1928.

Muhaidat RM, Sage RF, Dengler NG. 2007. Diversity of Kranz anatomy and biochemistry in C_4 eudicots. *American Journal of Botany* **94,** 362–381.

Nishioka D, Miyake H, Taniguchi T. 1996. Suppression of granal development and accumulation of Rubisco in different bundle sheath chloroplasts of the C_4 succulent plant. *Portulaca grandiflora. Annals of Botany* **77,** 629–637.

Nyffeler R, Eggli U. 2010. Disintegrating Portulacaceae: a new familial classification of the suborder Portulacineae (Caryophyllales) based on molecular and morphological data. *Taxon* **59,** 227–240.

Ogburn RM, Edwards EJ. 2009. Anatomical variation in Cactaceae and relatives: trait lability and evolutionary innovation. *American Journal of Botany* **96,** 391–408.

Poellnitz KV. 1934. Versuch eine Monographie der Gattung *Portulaca* L. *Feddes Repertorium* **37,** 240–320.

Porra RJ, Thompson WA, Kriedemann PE. 1989. Determination of accurate extinction coefficients and simultaneous equations for assaying chlorophylls *a* and *b* extracted with four different solvents: verification of the concentration of the chlorophyll standards by atomic absorption spectroscopy. *Biochimica et Biophysica Acta* **975,** 384–394.

Prabhakar M, Ramayya N. 1979. Anatomical studies in the Indian Portulacaceae. II. Leaf lamina. In: Periasamy K, ed. *Histochemistry, developmental and structural anatomy of angiosperms: a symposium*. Tiruchirapalli, India: P and H Publications, 159–169.

Pyankov VI, Artyusheva EG, Edwards G. 1999*a*. Formation of C_4 syndrome in leaves and cotyledons of *Kochia scoparia* and *Salsola collina* (Chenopodiaceae). *Russian Journal of Plant Physiology* **46,** 452–466.

Pyankov VI, Black CC Jr, Artyusheva EG, Voznesenskaya EV, Ku MSB, Edwards GE. 1999*b*. Features of photosynthesis in *Haloxylon* species of Chenopodiaceae that are dominant plants in Central Asian deserts. *Plant and Cell Physiology* **40,** 125–134.

Pyankov VI, Voznesenskaya EV, Kuz'min AN, Ku MSB, Ganko E, Franceschi VR, Black CC Jr, Edwards GE. 2000. Occurrence of C_3 and C_4 photosynthesis in cotyledons and leaves of *Salsola* species (Chenopodiaceae). *Photosynthesis Research* **63,** 69–84.

Ramayya N, Rajagopal T. 1974. Stomatogenesis in the genus *Portulaca* L. (Portulacaceae). *Botanical Journal of the Linnean Society* **68,** 81–88.

Rawsthorne S, Hylton CM, Smith AM, Woolhouse HW. 1988. Distribution of photorespiratory enzymes between bundle-sheath and mesophyll cells in leaves of the C_3–C_4 intermediate species *Moricandia arvensis* (L.) DC. *Planta* **176,** 527–532.

Rawsthorne S, Bauwe H. 1998. C_3–C_4 intermediate photosynthesis. In: Raghavendra AS, ed. *Photosynthesis. A comprehensive treatise*. Cambridge: Cambridge University Press, 150–162.

Sage RF. 2004. The evolution of C_4 photosynthesis. *New Phytologist* **161,** 341–370.

Samson R, Mani S, Boddey R, Sokhansanj S, Queseda D, Urguiaga S, Reis V, Lem CH. 2005. The potential of C_4 perennial grasses for developing global BIOHEAT industry. *Critical Reviews in Plant Sciences* **24,** 461–495.

Sheehy JE, Mitchel PL, Hardy B. 2007. *Charting new pathways to C_4 rice*. Los Banos, Philippines: International Rice Research Institute, World Scientific.

Sprey B, Laetsch WM. 1978. Structural studies of peripheral reticulum in C_4 plant chloroplasts of *Portulaca oleracea* L. *Zeitschrift für Pflanzenphysiologie* **87,** 37–53.

Sun J, Edwards GE, Okita TW. 1999. Feedback inhibition of photosynthesis in rice measured by O_2 dependent transients. *Photosynthesis Research* **59,** 187–200.

Thorne RF, Reveal JL. 2007. An updated classification of the Class Magnoliopsida ('Angiospermae'). *Botanical Review* **73,** 67–182.

Vogan PJ, Frohlich MW, Sage RF. 2007. The functional significance of C_3–C_4 intermediate traits in *Heliotropium* L.

(Boraginaceae); gas exchange perspectives. *Plant, Cell and Environment* **30,** 1337–1345.

von Caemmerer S, Farquhar GD. 1981. Some relationships between the biochemistry of photosynthesis and the gas exchange of leaves. *Planta* **153,** 376–387.

Voznesenskaya EV, Franceschi VR, Chuong SDX, Edwards GE. 2006. Functional characterization of phosphoenolpyruvate carboxykinase type C_4 leaf anatomy: Immuno, cytochemical and ultrastructural analyses. *Annals of Botany* **98,** 77–91.

Voznesenskaya EV, Franceschi VR, Pyankov VI, Edwards GE. 1999. Anatomy, chloroplast structure and compartmentation of enzymes relative to photosynthetic mechanisms in leaves and cotyledons of species in the tribe Salsoleae (Chenopodiaceae). *Journal of Experimental Botany* **50,** 1779–1795.

Voznesenskaya E, Koteyeva NK, Chuong SDX, Ivanova AN, Barroca J, Craven L, Edwards GE. 2007. Physiological, anatomical and biochemical characterization of the type of photosynthesis in *Cleome* species (Cleomaceae). *Functional Plant Biology* **34,** 247–1795.